PROCEEDINGS OF SCIENCE

Transverse single spin asymmetry measurement for very forward neutron production at the RHICf experiment

PoS(ICRC2023)525

Minho Kim[a,*]

[a] *RIKEN,*
Wako, Saitama, 351-0198, Japan

E-mail: minho.kim@riken.jp

In the high-energy $p+p$ collisions, the fundamental processes of extensive air shower development and hence the origin of the ultra-high energy cosmic ray can be studied by measuring the cross section of the very forward particles. On the other hand, transverse single spin asymmetry (A_{N}) for very forward particle production is an unique tool to understand the spin-involved diffractive particle production mechanism. A_{N} for very forward neutron production has been interpreted by an interference between π (spin flip) and a_1 (spin non-flip) exchange. Since the neutron A_{N} has been studied only in a narrow transverse momentum (p_{T}) range of $p_{\mathrm{T}} < 0.4$ GeV/c, the RHICf experiment measured the neutron A_{N} in a wide p_{T} coverage up to ~1 GeV/c to test the validity of the π and a_1 exchange model in the higher p_{T} region. In this poster, we report our analysis status and result on the neutron A_{N} measured by the RHICf experiment.

38th International Cosmic Ray Conference (ICRC2023)
26 July - 3 August, 2023
Nagoya, Japan

*Speaker

1. Introduction

In polarized $p+p$ collisions, transverse single spin asymmetry (A_N) is defined by a left-right cross section asymmetry,

$$A_\mathrm{N} = \frac{\sigma_\mathrm{L} - \sigma_\mathrm{R}}{\sigma_\mathrm{L} + \sigma_\mathrm{R}},$$

where the $\sigma_{\mathrm{L(R)}}$ is the cross section of a specific particle which is produced in the left (right) side with respect to the beam polarization. Since a large A_N for very forward ($\eta > 6$) neutron production has been discovered by a polarimeter development experiment [1], it has been measured by the PHENIX experiment at three different collision energies, 62, 200, and 500 GeV [2]. One pion exchange (OPE) model which had successfully described the cross section of the neutron production introduced an interference between the spin flip π exchange and spin non-flip a_1 exchange with a relative phase shift to reproduce the experimental data [3]. The π and a_1 exchange model reproduced the data well predicting that the A_N increases in magnitude with transverse momentum (p_T) with little longitudinal momentum fraction (x_F) dependence. Recently, the neutron A_N measured by the PHENIX experiment at $\sqrt{s}$ = 200 GeV was unfolded to precisely study the kinematic dependence of the neutron A_N and showed a consistency with the model prediction [4]. However, kinematic range of the experimental measurement and model calculation was narrow compared to that of very forward neutron production.

The RHICf experiment [5] measured the A_N for very forward neutron production in a wide p_T coverage of $0.0 < p_\mathrm{T} < 1.0$ GeV/c from polarized $p + p$ collisions at $\sqrt{s}$ = 510 GeV. The RHICf data allows us to test the validity of the π and a_1 exchange model in the higher p_T region. Since $\sqrt{s}$ of the RHICf experiment is different from those of previous measurements, one can also study the $\sqrt{s}$ dependence of the neutron A_N.

2. RHICf experiment

In June 2017, The RHICf experiment measured the A_N for very forward neutron production in polarized $p + p$ collisions at $\sqrt{s}$ = 510 GeV at the Relativistic Heavy Ion Collider (RHIC). An

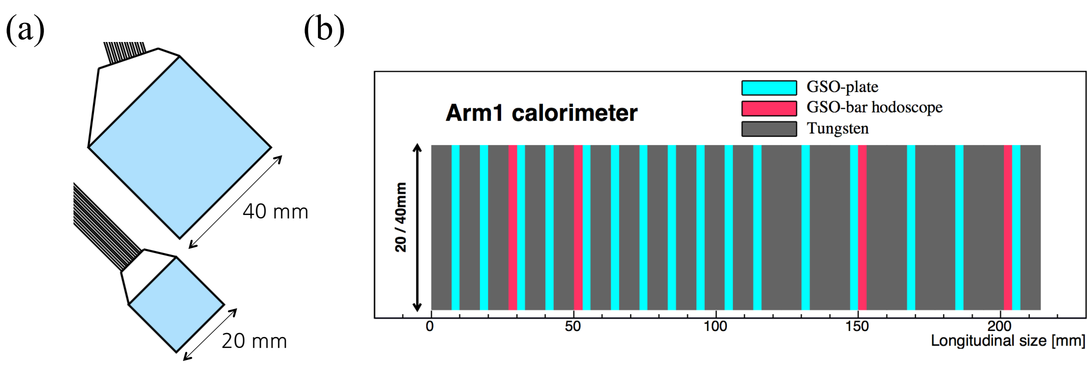

Figure 1: Schematic drawing of the (a) front view and the (b) longitudinal structure of the RHICf detector.

electromagnetic calorimeter (RHICf detector) [6] was installed in front of the STAR Zero-Degree

Calorimeter (ZDC) [7], which was located 18 m away from the beam interaction point. We also installed a thin scintillator counter (FC) in front of the RHICf detector to analyze the charged hadron background. Fig. 1 shows the schematic drawing of the RHICf detector. As shown in Fig. 1 (a), the RHICf detector consists of small and large sampling towers with 20 and 40 mm dimensions, respectively. They have same longitudinal structure as shown in Fig. 1 (b). Both towers are composed of 17 tungsten absorbers with 1.6 interaction length in total, 16 GSO plates for energy measurement, and 4 layers of GSO bar hodoscope for position measurement. Position and energy resolutions for 250 GeV neutron are about 1 mm and 39% when the incident position of the neutron is the center of a tower. A shower trigger which was operated when the energy deposits of three successive GSO plate layers are larger than 45 MeV was used for the neutron measurement. For more detailed detector configuration and performance, see Ref. [8], [9] and [10].

We requested large β^* value of 8 m at operation to make the angular beam divergence small. Corresponding luminosity at $\sqrt{s}$ = 510 GeV was $\sim 10^{31}$ cm^{-2}s^{-1} which was smaller than that in usual RHIC operation. We also requested a radial polarization which was 90°-rotated from that of usual RHIC operation to reach the maximal p_{T} range by moving the detector vertically. We took the data during about 28 hours with three detector positions where the beam headed the center of large tower, center of small tower, and 24 mm below the center of small tower.

3. Data analysis

Basically, only the shower triggered events were analyzed to avoid any bias from the different trigger efficiencies. The shower trigger is sensitive not only to the neutron events but also to the photon events. In order to separate the neutron events from the photon background, a cut condition of $L_{90\%} - 0.15L_{20\%} > 21$ was applied. $L_{x\%}$ is defined by longitudinal depth of detector where the accumulated energy deposit reaches x% of the total. The above condition was optimized taking into account the neutron purity and efficiency. Events where the hadronic shower developed in the deeper GSO plates were rejected by applying for $L_{90\%} < 37$ to improve the energy resolution of neutron. Energy resolution of 250 GeV neutron was improved from 39% to 30% accordingly.

Since the RHICf detector has insufficient interaction length for the neutron energy measurement, kinematic values of neutron were unfolded by using Bayesian unfolding [13]. For prior, a Monte Carlo (MC) sample where neutrons from 0 to 255 GeV were uniformly generated on the detector was used to avoid any bias from the particular particle productions. We repeated the iteration until the χ^2 change between two outputs of consecutive iterations became smaller than 1. Comparison between true, reconstructed and unfolded distributions of x_{F} and p_{T} values are depicted in Fig. 2. Neutron events of QGSJET II-04 sample were used for this comparison. One can see the unfolded distributions reproduce the true ones well. We generated finite asymmetry by assigning up and down spin patterns to each event and also confirmed that the unfolded distributions reproduced the input A_{N} well within the statistical uncertainty.

Background A_{N}s from the photon and charged hadron were subtracted using the following equation after unfolding,

$$A_{\mathrm{N}}^{\mathrm{neu}} = \left(\frac{N_{\mathrm{trig}}}{N_{\mathrm{neu}}}\right) A_{\mathrm{N}}^{\mathrm{trig}} - \left(\frac{N_{\mathrm{pho}}}{N_{\mathrm{neu}}}\right) A_{\mathrm{N}}^{\mathrm{pho}} - \left(\frac{N_{\mathrm{had}}}{N_{\mathrm{neu}}}\right) A_{\mathrm{N}}^{\mathrm{had}},$$

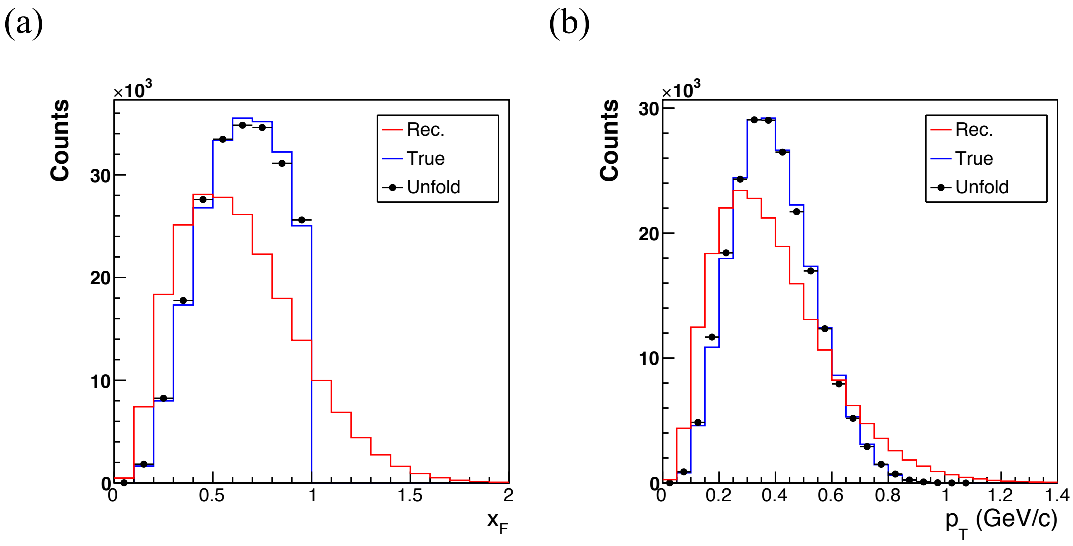

Figure 2: Comparison between the true, reconstructed and unfolded distributions of (a) x_{F} and (b) p_{T} values.

where the notations “neu", “pho", “had" and “trig" mean the neutron, photon, charged hadron and triggered events, respectively, and N is the number of measured events. Ratios between different types of events were estimated referring to the QGSJET II-04 sample. $A_{\mathrm{N}}^{\mathrm{pho}}$ was calculated using the photon-enhanced sample of data. In the preliminary result, the FC and $A_{\mathrm{N}}^{\mathrm{had}}$ were not analyzed, thereby A_{N} variation between when the value of $A_{\mathrm{N}}^{\mathrm{had}}$ was -1 and $+1$ was assigned as one of the systematic uncertainties. For additional sources of the systematic uncertainty, uncertainties of beam center calculation, polarization and unfolding were considered.

4. Results

Fig. 3 shows the preliminary result of the A_{N} for very forward neutron production. Fig. 3 (a) shows the neutron A_{N} as a function of p_{T} in different x_{F} ranges. In the two higher x_{F} ranges, the A_{N} increases in magnitude with p_{T} without x_{F} dependence as the model predicted. In $p_{\mathrm{T}} < 0.25$ GeV/c, they are consistent with those of PHENIX [4]. No $\sqrt{s}$ dependence was observed in the neutron A_{N}. A_{N}s in the lowest x_{F} range show different behavior compared to those in the higher x_{F} ranges, which indicates a x_{F} dependence that hasn't been expected by the π and a_1 exchange model. Fig. 3 (b) shows the neutron A_{N} as a function of x_{F} in different p_{T} ranges. In $p_{\mathrm{T}} < 0.25$ GeV/c, A_{N}s are flat without x_{F} dependence. However, in $p_{\mathrm{T}} > 0.25$ GeV/c, clear x_{F} dependence is observed.

In order to understand the x_{F} dependence of the neutron A_{N}, spin effect by an absorptive correction in the single π exchange was studied. The absorptive correction is an elastic interaction from the initial state proton or final state multi particles. Since phase shift by the absorptive correction starts to deviate from $p_{\mathrm{T}} \sim 0.3$ GeV/c, it has large A_{N} in the higher p_{T} region. Fig. 4 shows a comparison between the RHICf data and prediction by the absorptive correction in $0.46 < x_{\mathrm{F}} < 0.64$. The absorptive correction doesn't reproduce the RHICf data well. However, it shows a possible origin of the x_{F} dependence. Since the finite neutron A_{N} also comes from the π

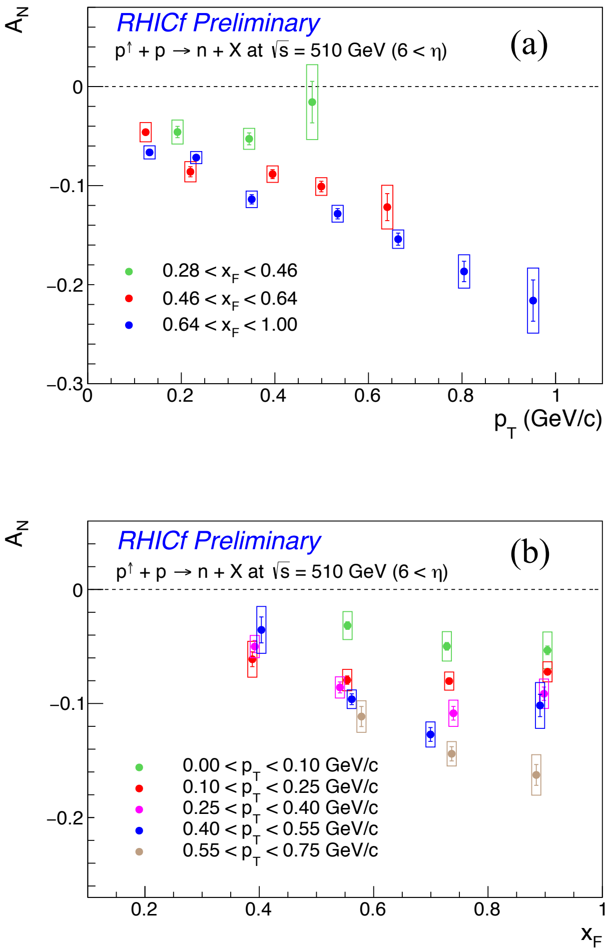

Figure 3: A_N for very forward neutron production (a) as a function of p_T in different x_F ranges and (b) as a function of x_F in different p_T ranges.

and a_1 exchange, we expect that more comprehensive theoretical calculation could reproduce the RHICf data.

To finalize the result, we analyzed the FC and the charged hadron background was suppressed by by rejecting the events where ADC of the FC has finite value. ADC distribution of the FC was reproduced in the simulation and effect of the charged hadron contamination after applying for the above condition was estimated. Since the background study has been recently completed, the final result of the neutron $A_{\rm N}$ will be released soon.

5. Summary

In June 2017, the RHICf experiment measured the $A_{\rm N}$ for very forward neutron production in polarized $p + p$ collisions at $\sqrt{s}$ = 510 GeV and presented the preliminary result. In $0.46 < x_{\rm F}$, the $A_{\rm N}$ increases in magnitude with $p_{\rm T}$ as the model predicted. No $\sqrt{s}$ was observed when the RHICf data points were compared with those of PHENIX result. In $p_{\rm T} < 0.25$ GeV/c, $A_{\rm N}$s are flat

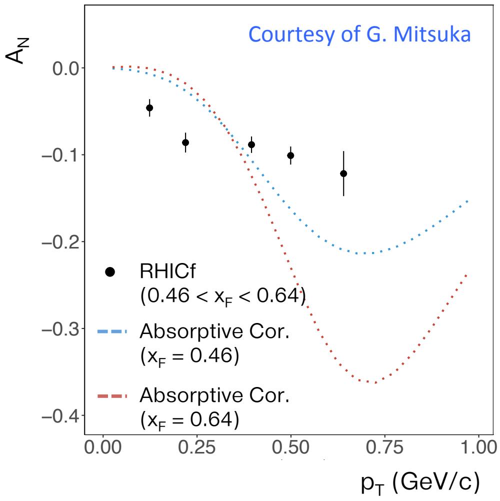

Figure 4: Comparison between the RHICf data and prediction by the absorptive correction in the single π exchange in $0.46 < x_F < 0.64$.

without x_F dependence. However, in $p_T > 0.25$ GeV/c, a clear x_F dependence was observed. In the preliminary result, effect of the charged hadron events was not analyzed in detail. However, since it has been complemented, we will finalize the result soon.

References

[1] Y. Fukao *et al.*, Phys. Lett. B **650**, 325 (2007).

[2] K. Tanida (PHENIX Collaboration), J. Phys. Conf. Ser. **295**, 012097 (2011).

[3] B. Z. Kopeliovich, I. K. Potashinikova, I. Schmidt, and J. Soffer, Phys. Rev. D **84**, 114012 (2011).

[4] U. A. Acharya *et al.* (PHENIX Collaboration), Phys. Rev. D **103**, 052009 (2021).

[5] RHICf Collaboration: LOI, arXiv: 1409. 4860v1.

[6] RHICf Collaboration, JINST **16** P10027 (2021).

[7] C. Adler *et al.*, Nucl. Instrum. Meth. A **470**, 488 (2001).

[8] T. Suzuki *et al.*, JINST **8**, T01007 (2013).

[9] Y. Makino *et al.*, JINST **12**, P03023 (2017).

[10] K. Kawade *et al.*, JINST **9**, P03016 (2014).

[11] M. H. Kim *et al.* (RHICf Collaobration), Phys. Rev. Lett. **124**, 252501 (2020).

[12] S. Ostapcheno, Nucl. Phys. B, Proc. Suupl. **151**, 143 (2006).

[13] G. D'Agostini, Nucl. Instrum. Meth. A **362**, 487 (1995).